Influence of external fields on spin reorientation transitions in uniaxial ferromagnets. II. Ultrathin ferromagnetic films

Y. T. Millev,* H. P. Oepen, and J. Kirschner
Max-Planck-Institut für Mikrostrukturphysik, Weinberg 2, D-06120 Halle, Germany
(Received 18 March 1997)

The field-dependent spin reorientation transition (SRT) in ultrathin ferromagnetic films is discussed. A rather general treatment is presented which involves the extension of the anisotropy-flow concept to systems in an applied magnetic field. Special features of field-induced SRT's are deduced from the general analysis. Emphasis is laid on the experimental implications, whereby general features are quantitatively described which are as characteristic as fingerprints and serve to set up a natural classification of the SRT's in external fields. Special attention is dedicated to resolving the substantial differences between in-field and spontaneous SRT's; ignoring these differences may result in grave misinterpretations of experimental findings. [S0163-1829(98)07809-6]

I. INTRODUCTION

In the preceding paper (to be denoted as I below),[1] we provided a detailed discussion of spin reorientation transitions (SRT's) in uniaxial systems under a field which is valid for both bulk and thin-film ferromagnets. A systematic discussion of the zero-field SRT in ultrathin films has been given very recently.[2] The general phenomenologic description requires further elaboration in the thin-film context, because one has to consider the influence of *shape* and *surface* anisotropies. It has been recognized long ago that the competition between these two and the bulk magnetocrystalline anisotropy underlies the SRT's in thin films.[3] The competition has a further dimension in the sense that higher-order anisotropies may also interfere significantly. The angular dependence of the relevant thermodynamic potential with field is the same for bulk and thin-film systems. However, the effective anisotropy constants a and b of the lowest two orders in thin films have an internal structure which makes the treatment in this case more complicated. As in I, complications arising due to domain formation will be neglected.

The dipolar effects can be described in terms of the demagnetization field. Assuming ideal planar geometry of the interfaces, one has a demagnetizing factor of 4π for the direction perpendicular to the surface,[4] whereas the factors within the plane are identically zero. Recent atomic-scale estimates of the demagnetization factors of ultrathin films can also be implemented; the deviations from the continuum values are significant for thicknesses of one and two monolayers only.[5] The important issue is that the dipolar contribution is restricted to the lowest anisotropy constant, because of symmetry considerations concerning the dipolar character of this source of anisotropy.[6]

The very important difference from the bulk case of a SRT is that the anisotropy constants vary with thickness. One thus has an extra ''degree of freedom'' in contrast to the bulk where the variations of anisotropy for a given system are almost invariably restricted to the temperature dependence of the anisotropy constants. For the thickness dependence of the anisotropy constants, one needs to introduce a further phenomenological assumption which has been proved to be of sufficient generality.[7–9] It is assumed that the surface and bulk contributions to a given anisotropy constant are additive with the surface contribution varying as the inverse thickness $(1/d)$.

With this assumption, the theoretical analysis of the thickness-driven SRT's is straightforward as has been shown for zero-field reorientations.[2] On the other hand, the analysis of temperature-driven SRT's in both bulk and thin-film systems is difficult to describe.[11] Nevertheless, a general conceptual framework for both thickness- and temperature-driven SRT's has been developed which is based on tracing down the evolution driven by the relevant parameter in the structured anisotropy space of the system.[12]

It must be emphasized that at a first glance the thickness dependence of anisotropy looks very similar to an aggravating circumstance which should make the description of anisotropy-dominated phenomena such as SRT's a very difficult task. However, the extra degree of freedom which is best exploited in wedge-shape geometry of the ferromagnetic films provides for an excellent possibility to study SRT's at fixed temperature and, indeed, gives the analysis of SRT's a really new dimension. The principal goals of our study are (i) to demonstrate that there exists a common basis for the analysis of both bulk and thin-film reorientations by homogeneous rotation of magnetization (part I), and (ii) to explore the implications of the thickness dependence for the SRT's. Thus, a variety of interesting phenomena can be predicted and described in sufficient detail within the thin-film context. These are the subject of the present paper. The instrumentals in the analysis will be the general representations obtained in I for coaxial and in-plane field configurations and the extension of the anisotropy-flow scheme to SRT's with external field. Note that the scheme with field has not been used in the bulk context either and there is no doubt that there it would illuminate better the related issues. This reverberation will not be pursued further in this study.

II. GENERAL BACKGROUND

To carry out the analysis, we need to specify the structure of the anisotropy constants a and b in the expression for the relevant thermodynamic potential[13] including the depen-

dence on the thickness of the film:

$$g_A = a\ \sin^2\theta + b\ \sin^4\theta - \mathbf{H}\cdot\mathbf{M}. \tag{1}$$

The angle θ is between the normal to the film and the direction of magnetization. The structure of the anisotropy constants is made explicit by the relations

$$a = -\Delta + \frac{K_{1s}}{d}, \tag{2}$$

$$b = K_{2b} + \frac{K_{2s}}{d}, \tag{3}$$

where $\Delta \equiv -K_{1b} + \frac{1}{2}(N_z - N_x)M^2$, K_{ib} and K_{is} with $i=1$ or 2 are the effective bulk and surface contributions to the magnetocrystalline anisotropy, while N_z and N_x are the demagnetization factors along the normal to the surface and along any axis within the plane. We neglect in-plane magnetocrystalline anisotropies, hence, the in-plane Descartes axes can be suitably chosen. In particular, we choose the x axis as the crossing line of the plane of the film with the plane where all three vectors **H**,**M** and the normal to the suface **n** lie. In the ideal continuum case, $N_z = 4\pi$, $N_x = N_y = 0$. In any case, for flat geometry which is at hand with ultrathin films N_x/N_z, $N_y/N_z \ll 1$ (see also Ref. 5). The dipolar contribution is contained in the quantity Δ and the special notation for it is justified by the fact that it is this combination of bulk and dipolar contributions which is relevant for the analysis. Clearly, the dipolar effect prefers to have the magnetization lying within the plane. Hence, perpendicular magnetization would only set in for strong enough surface anisotropy of a sign opposing the dipolar contribution. The surface anisotropies defined as in Eqs. (2),(3) encompass the contributions of both interfaces which are not equal, in principle. Rather generally, the anisotropies are functions of the temperature and of the thickness of the film $a = a(T,d)$, $b = b(T,d)$. In the following, we assume that one works at fixed temperature $T \ll T_C$; the temperature is treated as a parameter and will be suppressed. However, most of the important features of the analysis can be used at a fixed thickness and tunable temperature without modifications.

The important issues involved in the phenomenological ansatz of Eqs. (2),(3) for the structure of the anisotropy constants are the additivity of the bulk and surface contributions and the assumed $1/d$ dependence for the thickness-dependent part of the anisotropy.[14] On the technical side, the relations (2),(3) represent a *nonlinear*, but tractable transformation of the variables introduced in I to film-specific variables.

The inclusion of the second-order surface contribution is but natural, just as it is natural to include higher-order contributions in the bulk context. As already discussed before,[2] the most dramatic event at a SRT is the cancellation of the largest anisotropy contributions, i.e., first-order bulk, first-order surface, and dipolar contributions. Obviously, in the vicinity of such a point in thickness or temperature the anisotropy behavior of the system is stabilized and dominated by the first nonvanishing contribution and this is the second-order one, no matter how small it might appear against each of the principal competitors taken separately.[15] However, it is only recently that one has thought about the importance and the practical possibility to consider higher-order

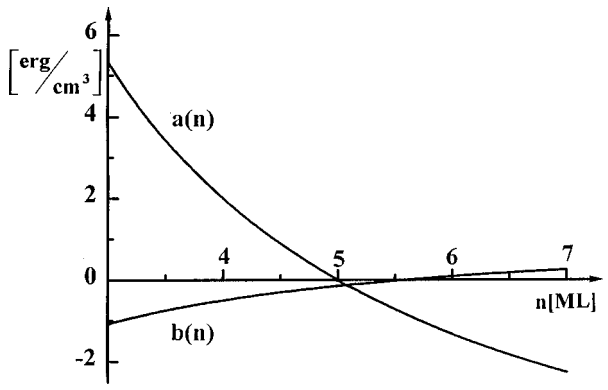

FIG. 1. Thickness dependence of the first two anisotropy constants a (solid curve) and b (dashed curve) for Co/Au(111). Thickness is given in monolayers (ML) ($1\text{ML} = 2\times10^{-8}$ cm). Around the point where a is zero ($n_0 = 5$ ML), the system is stabilized by the second-order contribution. Note a change of sign of b at a higher thickness.

anisotropies in ultrathin ferromagnetic films. Even this has taken shape in steps. Chappert and Bruno considered a second-order contribution but included only the bulklike part of it.[16] The same procedure was adopted by Grolier *et al.*[17] An attempt to consider K_{2s} systematically and to determine both bulk and surface anisotropy contributions from a single set of data was made by Fritzsche *et al.*[18] who used torsion oscillation magnetometry. A general analysis of spontaneous thickness- and temperature-driven SRT's in ultrathin films by means of the anisotropy-flow concept was presented in Ref. 2, while the insights provided by this general picture were very recently implemented[19] in the analysis of the magnetic microstructure of ultrathin wedges of cobalt on Au(111). The determination of the surface constants was performed on the basis of experimental data from scanning electron microscopy with polarization analysis of the secondary electrons.[20,21] The experimental findings of Ref. 19 seem to represent an unambiguous observation in ultrathin ferromagnetic systems of coexistence of coaxial and in-plane phases within a narrow range of thicknesses. Since the phenomenon of coexistence and the concommitant metastability effects have been in the focus of our general treatment of SRT's with external field in Ref. 1, it is instructive to have a practical example for the thickness dependence of the contributions to anisotropy coming from the different orders (Fig. 1). The curves for $a(d)$ and $b(d)$ refer to room temperature and have been obtained by using the results of the analysis for Co/Au(111).[19]

III. SYSTEMATICS OF POSSIBLE REORIENTATIONS IN APPLIED FIELDS

A substantial part of the problem is to typify on general grounds the behavior of thin films within a certain class of experiments which involve the implementation of an external field. Some peculiarities will be discussed which can be observed in thin films when their thickness is held constant, while the constant magnetic field may assume different magnitudes. Due to the thickness dependence of a and b [Eqs. (2),(3) and Fig. 1], the condition of constant thickness means that the ratio $r = a/b$ is constant as well. Hence, the experi-

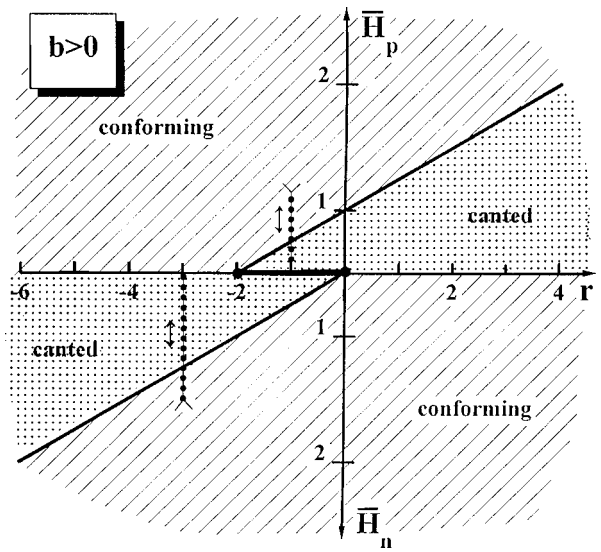

FIG. 2. Phase diagram for $b>0$. Both field configurations are envisaged in the same plot. $\overline{H_p}$ and $\overline{H_n}$ stand for in-plane and the vertical field configuration, respectively. The abscissa is $r(d)=a/b$. For a given thickness, $r=$const. The ordinate is the applied field normalized against the critical field $H_C=8|b|/M$. The dotted lines indicate the field variation for films of constant thickness belonging to definite generic regimes in the phase diagrams and typify the two distinct regimes of variation of M_H at fixed thickness [(a) $r<-2$ or $r>0$, (b) $-2<r<0$]. The corresponding magnetizations are given in Figs. 3 and 4.

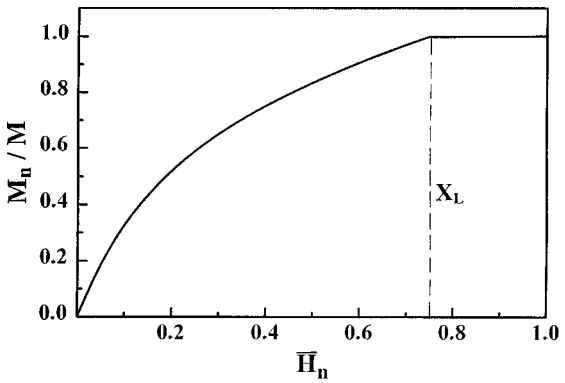

FIG. 3. Reversible continuous magnetization process for $b>0$ along the left dotted path in Fig. 2. A coaxial field is considered, but the curve is representative for both configurations and thicknesses corresponding to $r<-2$ or $r>0$. Field is normalized as in Fig. 2. Magnetization starts from zero at $\overline{H_n}=0$, since the stable spontaneous phase at $r<-2$ is in-plane. At the field strength marked by a dashed vertical line, a discontinuity of the first derivative occurs. At that field strength the vertical line in Fig. 2 ($r=-3$) traverses the phase boundary. This crossover points are denoted as X_L [cf. also Sec. V and Figs. 9(a), 9(b)].

mental situation is best represented in the $\overline{H}$ vs r diagram, already given in I. Following the classification with respect to the sign of b in zero field,[2] we have to distinguish between the following situations

A. Systems with a canted reorientation transition in zero field ($b>0$)

Figure 2 is similar to the plot shown in Fig. 3(a) of I. Investigating the behavior of a film of constant thickness in magnetic fields of different magnitude is equivalent to running along a vertical line through the plot. The film thickness determines the value of r where the line is located. The upper half of the diagram represents the situation with a magnetic field applied parallel to the film plane, while the lower half gives the experimental situation for a field along the surface normal. Two generic situations can be distinguished: (a) $r<-2$ or $r>0$ and (b) $-2<r<0$.

In the first case, starting from the r axis (no field applied), it is obvious that within the given ranges the coaxial ($r>0$) or the in-plane phase ($r<-2$) is stable, respectively. Switching on the field stabilizes the conforming phase, while a gradual tilt of magnetization appears when the field direction is perpendicular to the direction of spontaneous magnetization. Without loss of generality, we discuss as representative for this generic class a film with $r=-3$. The applied field is such that the system runs along the dotted line in Fig. 2(a). Figure 3 shows the magnetization component along the field direction when the field strength is varied in the configuration with the field parallel to the film normal. Upon increasing the field, the magnetization tilts more and more towards the direction of the applied field (Fig. 3). At a certain field strength, the magnetization becomes aligned with the external field. This point corresponds precisely to the reduced field where the phase boundary is crossed by the vertical line in Fig. 2. From Fig. 3 it is obvious that the transition is continuous, while the first derivative has a discontinuity. It is natural to denote such special points (fields) crossover points (fields). Generally, films of thicknesses belonging to r regimes of case (a) exhibit only one phase transition in each of both field geometries. This behavior indicates that the r value corresponds to a unique phase in zero field.

In the second case, $-2<r<0$, a ''true'' canted magnetization is found in zero field. Without the field, the canting angle varies along the abscissa with r between vertical alignment at $r=0$ to in-plane alignment of magnetization at $r=-2$. Switching on the external field causes in both field configurations a further magnetization tilting towards the direction of the field. This is shown in Fig. 4 for the dotted line at $r=-1$ in the phase diagram (Fig. 2) for the case of in-plane field orientation. A magnetization profile such as the one in Fig. 4 can be found for the case of a vertically applied field. Hence, in both field configurations a phase boundary appears which corresponds to the locus of points where the magnetization orientation becomes collinear with the field direction. The transition is once again continuous, while the first derviative is discontinuous. The appearance of two phase boundaries (one per field configuration) implies values of r for which a ''true'' SRT via the canted phase is found in zero field. The ratio of the field strengths at the phase boundaries correlates directly with the value of r and can be used to determine r as a function of film thickness.

B. Systems with a reorientation transition via the phase of coexistence in zero field ($b<0$)

The plot in Fig. 5 is equivalent to the plot for $b<0$ shown in Fig. 3(b) of I. Three different generic cases have to be

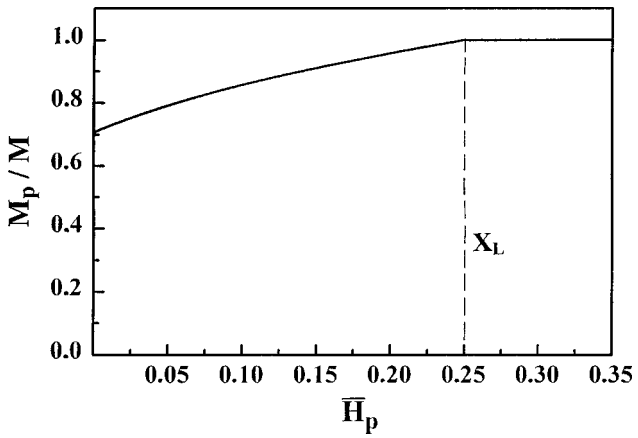

FIG. 4. Reversible continuous magnetization process for $b>0$ along the right dotted path in Fig. 2. In-plane field is assumed, but the curve is typical for both configurations for $-2<r<0$. The field is normalized as in Fig. 2. A transition is marked by a vertical dashed line, labeled by X_L again. The first derivative is discontinuous. The magnetization does not vanish in zero field, since the system evolves from the ''true'' zero-field canted phase.

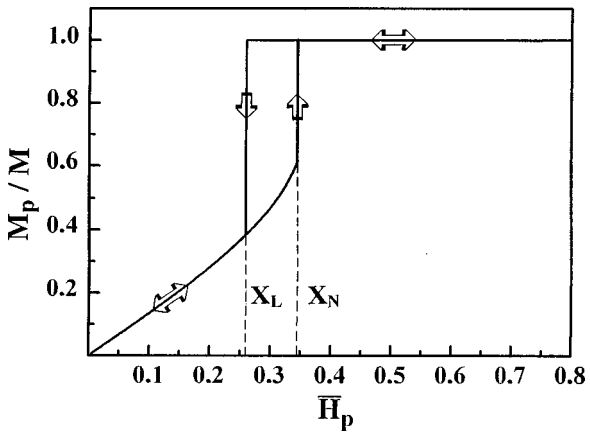

FIG. 6. Hysteresis for $b<0$ on varying the field along the dotted line at $r=-3$ in Fig. 5. Arrows show the direction of change of applied field. Jumps in magnetization correspond to discontinuous first-order transitions at the cross points of the chosen path with the two phase lines bounding the region of coexistence. The two points can only be revealed if the two directions of change of field are scanned. X_L (X_N) is a linear (nonlinear) crosspoint [see Sec. V and Figs. 9(a), 9(b)].

considered in this situation: (a) $r<-6$, $r>4$, (b) $-6<r<-2$, $0<r<4$, and (c) $-2<r<0$.

In the first case ($r<-6$, $r>4$), the scenario that can be observed under field variation is identical to the situation discussed as a first case for $b>0$ above. In the second case ($-6<r<-2$, $0<r<4$), remarkable deviations from the situation with $b>0$ can be found as the region of coexistence

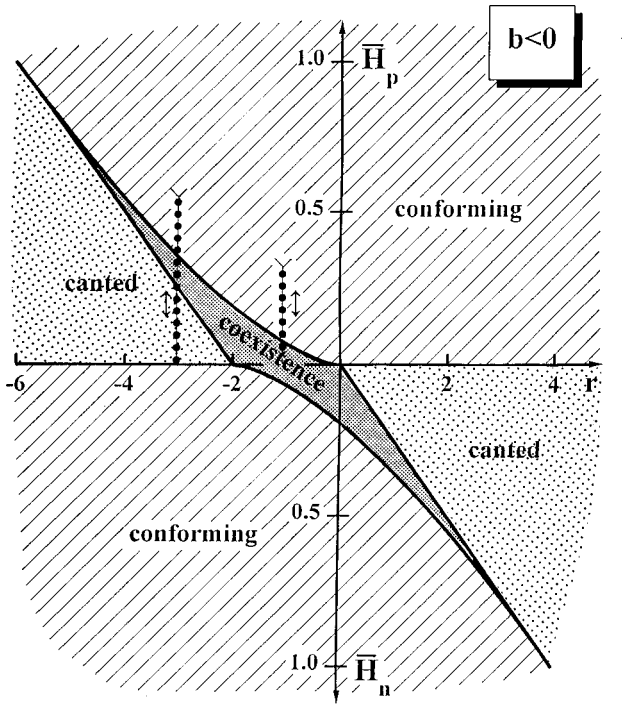

FIG. 5. Phase diagram for $b<0$. Both field configurations are ''glued together'' at the abscissa $r=a/b$. There are three distinct regimes: (a) $r<-6$ or $r>4$, (b) $-6<r<-2$ or $0<r<4$, and (c) $-2<r<0$. The first type is akin to the first type with $b>0$ (Fig. 2). For the remaining two, typical paths (dotted lines) are chosen. The situation is drastically different from the one with $b>0$, since the region of coexistence is being traversed (cf. Figs. 6 and 7).

persists over a range of applied field strengths. Two phase boundaries appear in each configuration on varying the magnetic field in the direction perpendicular to the spontaneous magnetization orientation (cf. dotted line at $r=-3$ in Fig. 5). Between the two crossover fields the region of coexistence appears where the conforming and canted phases are both stable and represent local minima of the free enthalpy. It must be emphasized that the thicknesses where these field effects are found belong to the thickness regime where in zero field one out of two phases (collinear or in-plane) is stable. The fact that coexistence shows up on field variation gives rise to hysteresis effects. Due to the stability of both the conforming and canted phases within that peculiar field regime, the phases on either side persist when crossing their boundary to the region of coexistence. The consequence is that two different crossover fields appear depending on whether the field is increased or decreased which is illustrated by Fig. 6. The plot shows the in-plane magnetization component as a function of in-plane field strength at $r=-3$. The canting angle increases with field. As the canted phase is stable up to the higher crossover field, there are no discontinuities at the lower crossover field. At the phase boundary to the conforming phase, denoted as X_N in Fig. 6, the canted phase can no longer be sustained. The magnetization has to turn abruptly into an in-plane orientation and this results into a discontinuous transition. The conforming phase is the only stable one in higher fields. When the field is decreased, starting from within the conforming phase, the latter is stable across the whole coexistence regime. A discontinuous change to canted magnetization occurs at the phase boundary (X_L in Fig. 6) to the canted phase. This behavior causes the hysteresis shown in Fig. 6. Both crossover fields manifest themselves as discontinuities in the components of the thin-film magnetization. Such behavior was discussed in the context of SRT's in bulk systems.[22]

In the third case, $-2<r<0$, coexistence is found even in zero field. With the field, the film will manifest a very strange behavior. In both field configurations it exhibits the

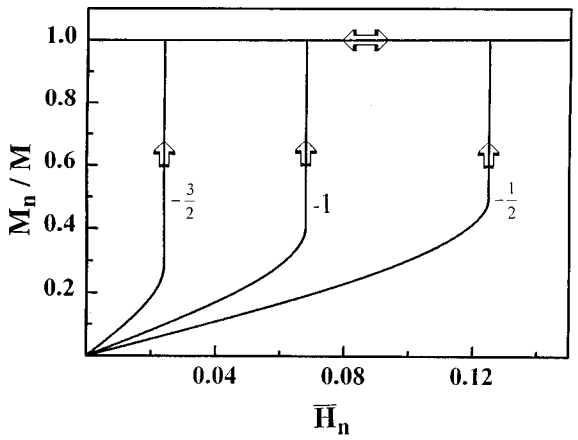

FIG. 7. Hysteresis for $b<0$ at $r=0.5,\ -1,\ -1.5$ representing the generic case given by the dotted line at $r=-1$ in Fig. 5. The plots are similar in both field configurations [$M_n(M_p)$ vs $H_n(H_p)$]. Starting from a ''true'' zero-field region of coexistence brings about a discontinuous transition on increasing the field. Upon decreasing, the magnetization remains caught in the respective conforming state (see text).

conforming-phase behavior. As soon as the film has been driven into the respective conforming phase by a magnetic field of sufficient strength, it will stay in this phase, because no line of instability for this conforming phase will be encountered under any field variation in that field geometry. When the configuration is changed to its orthogonal, a single transition emerges (Fig. 7) for different r values within this particular interval in r. On increasing the field the magnetization is tilted up to the crossover field where it flips to the conforming phase.

As a corollary, the field variation allows a general classification of the properties of ferromagnetic films when considering the crossover fields which can be observed. In addition, the type of phase transition offers an immediate opportunity to carry out a classification according to the sign of b. Hence, the systematics can be used as a fingerprint characteristics of the evolution of a thin-film system under variation of the film thickness.

IV. THE ANISOTROPY-FLOW CONCEPT FOR ULTRATHIN FILMS IN APPLIED FIELD

An important part of our general presentation of the problem of SRT's in ultrathin films with field is discussed in the present section. We follow the procedure of Ref. 2 and eliminate the thickness to remain with a *linear* functional connection between the first and second anisotropy constants.[14] We introduce the variables (α,β) which are the most suitable ones for the description of the thickness-driven anisotropy flows with field [Eqs. (29),(30) in I]. The linear relationship between the anisotropy constants is not affected at all by the normalization against the Zeeman amplitude. It takes on the appearance

$$\beta=\frac{\kappa_{2s}}{\kappa_{1s}}\alpha+\left(\frac{\kappa_{2s}}{\kappa_{1s}}\delta+\kappa_{2b}\right) \tag{4}$$

or

$$\alpha=\frac{\kappa_{1s}}{\kappa_{2s}}\beta-\left(\frac{\kappa_{1s}}{\kappa_{2s}}\kappa_{2b}+\delta\right), \tag{5}$$

where the notations $\delta=\Delta/HM$ and $\kappa_\mu\equiv K_\mu/HM(\mu=1b,2b,1s,2s)$ have been used.[23]

It is a most important recognition that the linear trajectory of Eq. (4) is *independent of the field configuration (coaxial or in-plane).* This means that for any given system specified by the set of anisotropy parameters $\{\kappa_\mu\}$ and δ the corresponding trajectory is rigidly bound to the (α,β) frame of reference regardless of the field configuration. What changes from configuration to configuration is the *structure* of the (α,β) space and this has been determined by the stability analysis of I [cf. Figs. 3(a), 3(b) therein]. In other words, placing an ultrathin film from a coaxial field configuration with some field $\mathbf{H}_n$ to an in-plane configuration with a field $\mathbf{H}_p$ such that $|\mathbf{H}_n|=|\mathbf{H}_p|=H$, we change the scenery (phase boundaries), but do not affect the trajectory in the (α,β) space.[24] This is a very useful property of the discussed representation, especially when combined with further features which we now describe.

As noted above,[23] for a given system *the slope of any trajectory is independent of the field and equals the ratio* K_{2s}/K_{1s}. This has an immediate important consequence. Trajectories corresponding to different field magnitudes are *parallel to each other regardless of the field configuration.* Thus, continuous variation of field corresponds to an infinite family of parallel trajectories of slope K_{2s}/K_{1s} (when β is the ordinate and α is the abscissa).

On the other hand, for a given system the intercept with the ordinate of any trajectory is inversely proportional to the field in each of the field configurations. From Eq. (4) it follows that

$$\frac{\kappa_{2s}}{\kappa_{1s}}\delta+\kappa_{2b}=\frac{(K_{2s}/K_{1s})\Delta+K_{2b}}{HM}\sim\frac{1}{H}. \tag{6}$$

For $H\to 0$, the intercept and the trajectory itself go to infinity in accordance with the remark in I that the zero-field (spontaneous) case cannot be ''observed'' in this presentation. For $H\to\infty$, the intercept goes to zero from above or below depending on the sign of the intercept. As with the *slope* commented on above, the *sign* of the intercept is independent of the magnetic field. Hence, for a given system the sign of the intercept and the slope are invariants of this representation and do not depend on the magnitude of the applied field for either coaxial or in-plane field.

In the discussed physical context thickness-driven flows, while linear, are bound to connect definite initial (α_i,β_i) and final (α_f,β_f) states corresponding to certain initial (d_i) and final (d_f) thicknesses. That is, each trajectory is, in fact, a segment of a line whose slope and sign of intercept are insensitive to field variations. By virtue of the definition of the quantities α and β, both initial and final states are inversely proportional to H, i.e., $\alpha_i(H),\beta_i(H),\alpha_f(H),\beta_f(H)\sim 1/H$. Consequently, the set of initial states and the set of final states are two lines going into the origin for $H\to\infty$.

The behavior of an ultrathin film can now be described for any magnitude of field by the following construction which we choose to discuss for the vertical field configuration without any loss of generality (Fig. 8). Consider the anisotropy

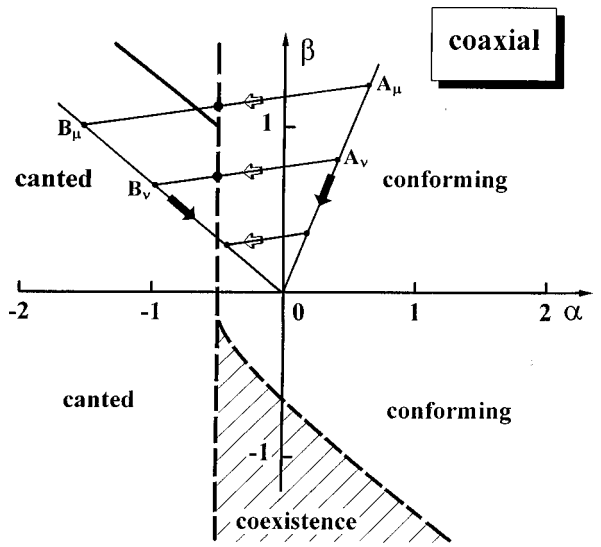

FIG. 8. Anisotropy-flow construction (coaxial field configuration). The thickness-driven trajectories are linear between initial (A_μ) and final (B_μ) states. Hollow arrows: increase of d. Black arrows: increase of applied field. For a given system, slope and sign of intercept are invariants. Beam OA (OB) corresponds to constant initial (final) thickness in different fields. Segments $\{A_\mu B_\mu\}$ are isolines of constant field under variation of thickness.

space and assume that all information for the initial and final states is known. These are then represented by two points, say, A_μ and B_μ in the (α,β) plane. For definiteness, A_μ is chosen to correspond to the smaller thickness. Draw the beam OA. All initial states which differ only by the magnitude of H lie along OA; the greater the field, the closer to the origin the initial state is. All points along OA correspond to the *same* initial thickness d_i. Draw the beam OB. All final states lie along it and correspond to the *same* final thickness d_f. The trajectory described by the system under variation of thickness (thickness-driven anisotropy flow) is the line connecting A_μ and B_μ for the initially chosen field H_1. For any other magnitude of field, say, H_2, the trajectory is given by a segment parallel to $A_\mu B_\mu$ as the slope K_{2s}/K_{1s} is independent of the field. Starting off at, say, A_ν, one obtains immediately the corresponding end point B_ν. Furthermore, $OA_\mu/OA_\nu = OB_\mu/OB_\nu = H_2/H_1$. The arrows on the beams OA and OB in Fig. 8 correspond to initial and final states in ever larger fields. The origin is the asymptotic point where the field is so strong (infinitely strong) that the difference in thickness between the states $\{A\}$ and the states $\{B\}$ no longer matters.

All this information can be concisely summarized by the claim that the isolines of constant thickness are represented by the family of beams flowing into the origin with increasing field, while the isolines of constant field are given by the family of parallel segments $\{A_\mu B_\mu\}$. *These are the possible thickness-driven trajectories*. The representation can thus be used in various ways as a predictive tool in accordance with the information given and/or required. In particular, one can easily delineate the region where the system is allowed to evolve and determine under what conditions, if at all, a region of coexistence would be traversed or just invaded. Altogether, on comparison with the zero-field case[2] one observes a greater variety of possibilities due to the additional variable (applied field) which are still held under control and can be systematized by projecting the anisotropy-dominated physics of the SRT onto the suitably chosen (α,β) space.

V. CROSSOVER THICKNESSES FOR SPIN REORIENTATION TRANSITIONS IN APPLIED FIELDS

A. Defining equations

A crossover thickness is naturally defined as corresponding to the border point where a given trajectory crosses a given phase borderline. We have presented evidence that the (α,β) diagram with its linear trajectories is best suited for a general analysis of thickness-driven SRT's. It appears self-suggesting [Figs. 9(a), 9(b)] to classify the possible scenarios for the evolution of the system according to the number of crossover thicknesses which go together with a given linear trajectory. Thus, there are *four* typical trajectories for each of the two configurations. The types are distinguished by zero, one, two, or three cross points of the relevant trajectory with the phase borderlines. The case of no cross points is irrelevant to a discussion of SRT's. In Fig. 9, the trajectories join initial (ξ) and final (η) states belonging to different phases in the diagram. Examples are given for classes of trajectory with different numbers of cross points. The arrows indicate the increment of thickness as a driving parameter.[25] For the determination of the crossover thicknesses at the given crossover it suffices to notice that these are deduced from only two distinct conditions, a linear one for a cross point of a trajectory with the linear phase boundary and a nonlinear one for a cross point with the nonlinear boundary. We denote generically the cross points (X points) of the first and second types as X_L and X_N, respectively (L for linear, N for nonlinear).

For the *coaxial* field configuration, the defining equation for the crossover thickness d_L corresponding to a cross point of the type X_L is [cf. Eq. (32) in I]:

$$\alpha(d_L) = -\frac{1}{2}, \tag{7}$$

while d_N for a cross point of the type X_N is found by Eq. (34) in I as

$$\alpha(d_N) = -2\beta(d_N) + \frac{3}{2}[\beta(d_N)]^{1/3}. \tag{8}$$

For the *in-plane* field configuration, d_L for X_L is defined by Eq. (37) in I

$$\alpha(d_L) + 2\beta(d_L) = \frac{1}{2}, \tag{9}$$

while d_N for X_N is given by Eq. (39) of part I

$$\beta(d_N) + \frac{8}{27}\alpha^3(d_N) = 0. \tag{10}$$

For a given system specified by the values of the material parameters $K_\mu(\mu = 1b, 2b, 1s, 2s)$ and M and by virtue of the *Ansätze* (2),(3), all of the above equations, when solved for d_L or d_N, give the experimentally very important *field*

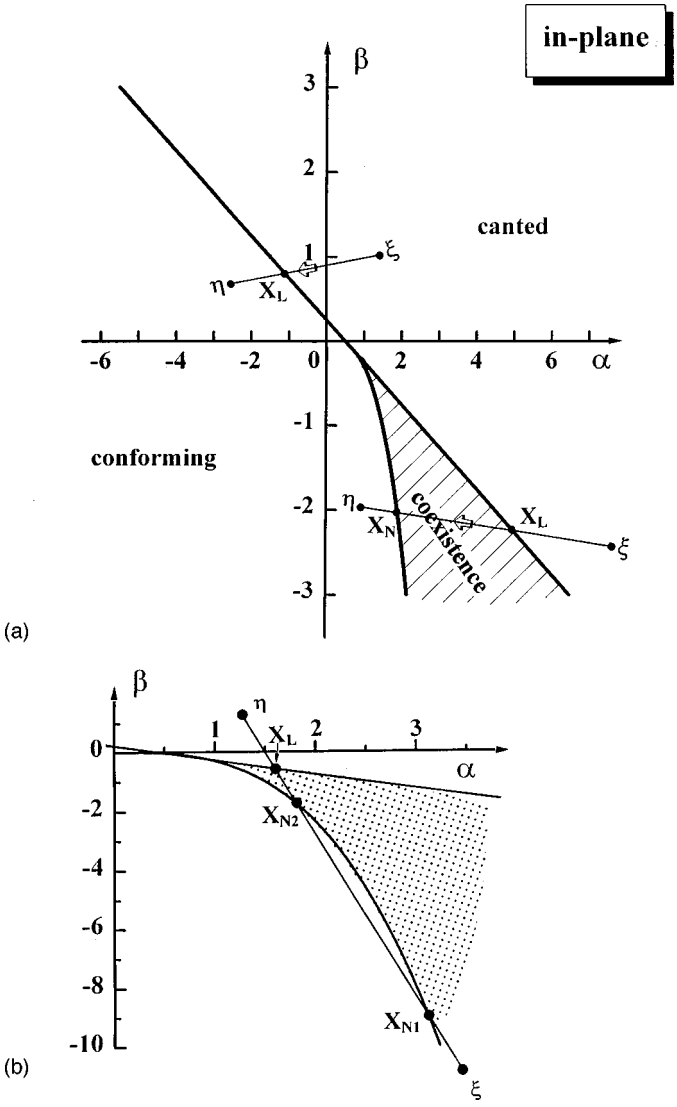

FIG. 9. Classification of possible scenarios for thickness-driven evolution according to the number of crossover points X of possible trajectories with phase boundaries (illustrated for the in-plane configuration). For a system with a SRT, one, two, or three crossover points are possible. $\xi(\eta)$ is an initial (final) point of a trajectory corresponding to a smaller (larger) thickness. $X_L(X_N)$ are cross points with a linear (nonlinear) boundary. (a) Regimes with *one* or *two* cross points. (b) Regime with *three* crossover points, two of which are of the X_N type. This regime is very peculiar and can only be realized with a starting point within the region of coexistence. Note a suitable change of scale for β in panel (b).

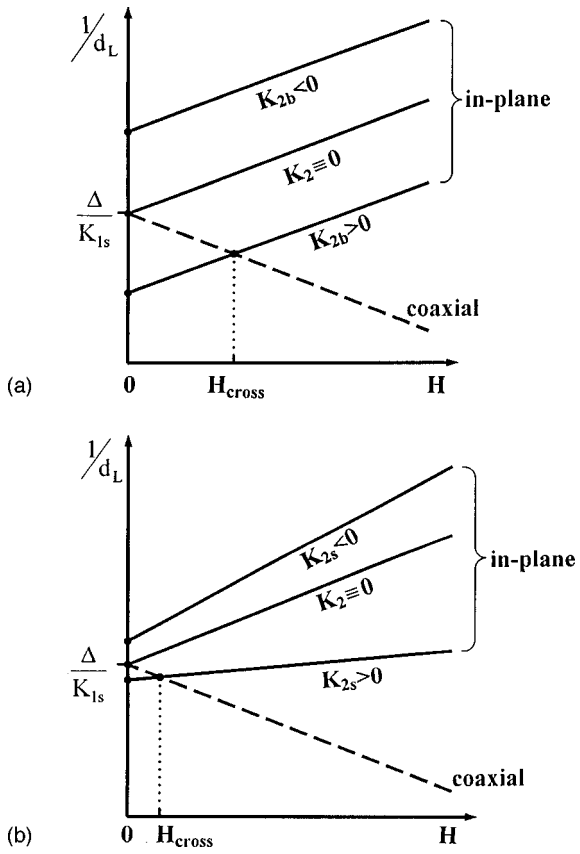

FIG. 10. Plot of $1/d_L$ vs field for $K_{1s}>0$. The crossover thicknesses are given for coaxial and in-plane magnetization orientation. (a) demonstrates the impact on $1/d_L$(in-plane) of varying K_{2b} at $K_{2s}=0$, while (b) illustrates the influence of K_{2s} at $K_{2b}=0$. In the in-plane configuration, the change of the intercept upon variation of K_{2b} is $\Delta I_1=|2K_{2b}/K_{1s}|$ (a); for the case of (b) this is $\Delta I_2=|2\Delta/(K_{1s}+2K_{2s})|$. At a certain field H_{cross}, given in Eq. (15), it is possible to obtain the same crossing thickness in both field configurations if $b>0$.

dependence of the crossover thicknesses in both field configurations. As emphasized above, the d_L's and d_N's come from the solution of a linear or nonlinear (cubic) equation, respectively. The explicit solutions of the arising cubics are difficult to handle analytically; in any case, they are given by the formulas in the Appendix of I which apply for the reduced form of any cubic. On the contrary, the *linear* crossover thicknesses d_L (coaxial) and d_L (in-plane) as defined in Eqs. (7) and (9) are both simple and informative. We discuss their practical significance and some self-suggesting applications in the next section.

Let us comment briefly on the possibility of *three* crossover points existing for both field configurations and illustrated for the in-plane configuration by the trajectory $\xi\eta$ in Fig. 9(b). A line and a segment can only cross at a single point if at all, hence, only one of the crossover points is of the linear type (X_L). d_L is given by Eq. (9). The remaining two cross points are of the nonlinear type (X_N) and are denoted in Fig. 10 as X_{N1} and X_{N2} in the order of increasing thickness. The corresponding crossover thicknesses d_{N1} and d_{N2} obey the cubic Eq. (10). That is to say, for specific systems whose linear trajectories do have two nonlinear cross points the relevant cubic equation has two physically relevant solutions d_{N1} and d_{N2}. This regime can be realized only with starting points within the region of coexistence. Its existence implies an anomalously large second-order surface contribution, since the typical slope of a prospective trajectory as the one given in Fig. 9(b) is large.

Formally, the above considerations about the location of the X points may be summarized in a description by means of plane analytic geometry of the points where a curve (the trajectory) crosses two other curves (the phase boundaries), the types of all curves being known. The fact that two of the curves involved are straight lines facilitates the analysis and, together with the explicit *Ansätze* for the $1/d$ dependence, leads to tractable equations for the crossover thicknesses.

However, the concept would work qualitatively even if the trajectory and/or the borderlines are given by more complex expressions or are implicit. This is the case one encounters with the temperature-driven trajectories for bulk anisotropy which are given by implicit expressions;[10,26] the same should be expected for temperature-driven SRT's in ultrathin films.[10,11] Furthermore, geometrically possible points where trajectories are *tangent* to borderlines can be expected to give rise to peculiar behavior detectable in experiments on SRT's. By inspection of our phase diagrams, there is a whole family of physical trajectories tangent to the cubic parabola. The consequences will not be pursued further here.

B. Field dependence of the linear crossover thickness d_L

By Eqs. (7) and (9) implemented together with the *Ansätze* (2),(3), one finds for the two principal field configurations that

$$\text{coaxial:}\frac{1}{d_L}=\left[-\frac{M}{2K_{1s}}\right]H+\frac{\Delta}{K_{1s}}; \tag{11}$$

$$\text{in-plane:}\frac{1}{d_L}=\left[\frac{M}{2(K_{1s}+2K_{2s})}\right]H+\left[\frac{\Delta-2K_{2b}}{K_{1s}+2K_{2s}}\right] \tag{12}$$

with Δ defined after Eq. (3). Thus, in both cases $1/d_L$ is proportional to H. Consequently, the $1/d_L$ vs H plots would be linear with the specified slopes and intercepts. Note that the overall sign of the slope depends crucially on the signs of the surface constants. The intercepts are identified as the zero-field characteristic thicknesses of Ref. 2. It is suitable to introduce the notation $d_0 \equiv d_L(H=0)$, hence,

$$d_0(\text{coaxial})=K_{1s}/\Delta, \tag{13}$$

while

$$d_0(\text{in-plane})=(K_{1s}+2K_{2s})/(\Delta-2K_{2b}). \tag{14}$$

Equations (11),(12) allow a general classification of the field dependence of the crossover thickness d_L. Mind that we have focused on systems where a thickness-driven SRT exists. This requirement is equivalent to demanding the anisotropy flow to cross the ordinate in the zero-field $(\widetilde{K}_1-K_2)$ representation of Ref. 2. Mathematically, this means that $K_{1s}\Delta>0$ which restricts the manifold of possible cases to be considered for the coaxial configuration [Eq. (11)] to a unique generic behavior. In every situation a positive intercept is found while the variation with field strength can have positive or negative slope depending on the sign of the surface contribution to the first anisotropy constant. The above requirement is manifest in the existence of d_L (coaxial) over a certain field range, at least. In the case of positive K_{1s} corresponding to a SRT from vertical to in-plane orientation upon increase of thickness, the slope is negative and the crossover thickness goes to infinity as the field approaches the value $H=2\Delta/M$. As already emphasized above, d_L (coaxial) in Eq. (11) is independent of the second-order anisotropy contribution b. We develop the discussion for positive K_{1s} without loss of generality. In Fig. 10 the dashed line denoted as ''coaxial'' represents the situation for the vertical-field configuration. To demonstrate the influence of the individual higher-order contributions upon the graph for $1/d_L$ (in-plane), we consider switching K_{2b} or K_{2s} on and off.

If $b=K_2=0$, the intercepts $1/d_0$(in-plane) and $1/d_0$(coaxial) are identical and the slopes have opposite signs (Fig. 10). The very existence of only one crossover thickness in zero field is consistent with the model of the first-order SRT that should be expected if higher-order anisotropies are neglected.

Switching K_{2b} on [Fig. 10(a)], while keeping K_{2s} equal to zero, does not bring about any change of the slope compared to the former case with $b=0$. The intercept, however, is modified. It becomes larger (smaller) for negative (positive) signs of K_{2b}. Again the dependence of the zero-field value $1/d_0$ (in-plane) on the sign of K_{2b} is consistent with the behavior which one should expect for a spontaneous SRT. For $K_{2b}>0$, the phase boundary between ''true'' canted and in-plane magnetization appears at higher thicknesses than the boundary separating ''true'' canted from vertical phases (for $K_{1s}>0$). As the slope is unaffected by the inclusion of K_{2b}, one obtains three parallel lines which typify the effect of an arbitrary nonzero value of K_{2b}.

The similarity to the zero-field case is not held up if one takes the coaxial behavior into consideration. Obviously, depending on the sign of K_{2b}, one can identify either a crossing of the lines $1/d$ (coaxial) and $1/d$ (in-plane) or a situation in which the inverse crossover thicknesses run away from each other. Films with negative K_{2b} will never exhibit crossover thicknesses which are identical in both field geometries at some field strength H_{cross}. For positive values of K_{2b}, there always exists a field strength H_{cross} at which identical crossover thicknesses can be observed in the different configurations. In particular, for $K_{2b}=0$ this field strength is zero.

Now assume that $K_{2s}\neq 0$, while K_{2b} vanishes identically [Fig. 10(b)]. Changes in both intercept and slope result. Once again for $K_{2s}>0$ one finds a decrease of intercept as compared with the coaxial case. The slope becomes smaller compared with the case $b=0$. The slope becomes vanishingly small in the limit $K_{2s}\to\infty$ which is synonymous to no SRT at all. For $K_{2s}<0$, the intercept and the slope increase. As in the former case, a crossing field H_{cross} exists for $K_{2s}\geqslant 0$; this again corresponds to the situation when in zero field the thickness-driven trajectory traverses the ''true'' canted phase.

As the $1/d_L$ linear plots have slopes of opposite signs for the different field configurations, one can generally expect the existence of a crossing field with identical crossover thicknesses if the intercepts fulfil the condition $1/d_0(\text{coaxial})>1/d_0(\text{in-plane})$ in the case with $K_{1s}>0$. Vice versa, whenever the last inequalities are fulfilled, the system will exhibit an exchange of ordering of crossover points at some higher field H_{cross}. These zero-field conditions for the crossover thicknesses are identical with those defining the boundaries of the ''true'' canted phase.[27] Hence, one can conclude that the field dependence of the crossover thicknesses will lead to the existence of a crossing field if a SRT via the ''true'' canted phase exists in the thin-film system in zero field. From Eqs. (11),(12) one obtains

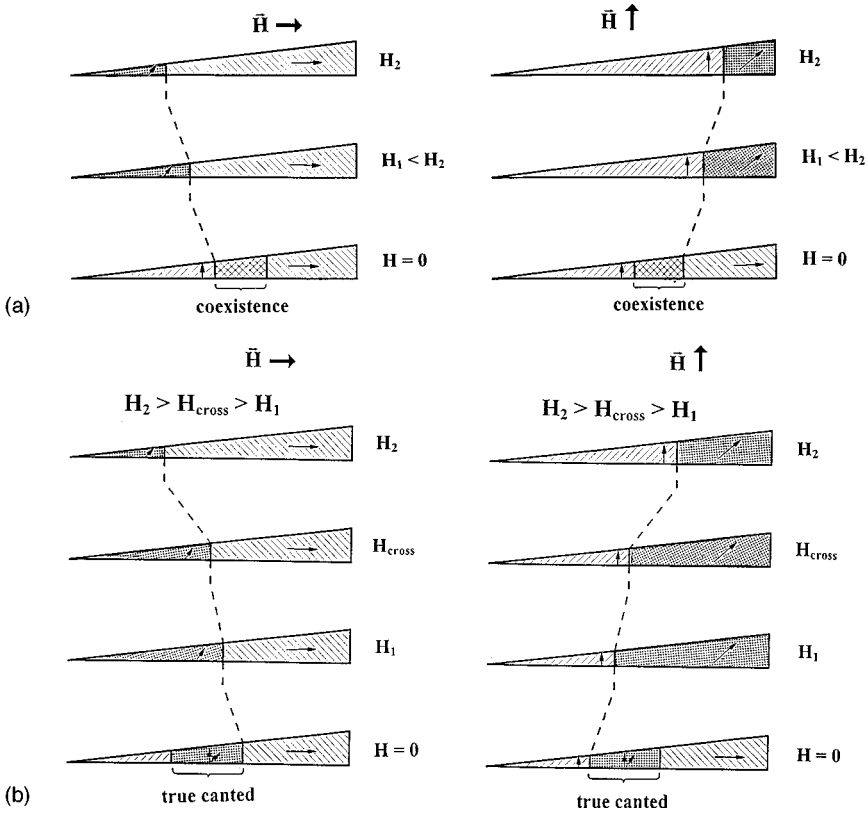

FIG. 11. Evolution of crossover thicknesses on a wedge upon increasing the field from zero. (a): systems exhibiting coexistence of phases in zero field (bottom wedge). Panel (b): systems exhibiting a true canted phase in zero field (bottom wedge). The in-plane field configuration is presented to the left, the vertical one is to the right in each of the panels. For nonzero field, the two competing phases (canted and conforming) are denoted as dotted and hatched regions on the wedge. The crossover thicknesses between these two phases evolve as described in text [see also Figs. 10(a), 10(b)]. For systems of type (a), the crossover thicknesses in the different configurations run away upon increasing the field. For those of type (b), the crossover thicknesses move closer starting from $H=0$, get equal at $H=H_{\rm cross}$, and run away for $H>H_{\rm cross}$.

$$H_{\rm cross}=\frac{2(\Delta K_{2s}+K_{2b}K_{1s})}{M(K_{1s}+K_{2s})}. \tag{15}$$

On the other hand, if the spontaneous SRT proceeds via the phase of coexistence,[2] a crossing field strength does not exist.

Figures 10(a), 10(b) are very instructive for the discussion of certain classes of experiments where the thickness-dependent behavior is studied in applied field. The detection of a SRT by the respective crossover thickness and the proper interpretation of the latter can now be effected with ease. The variation of thickness corresponds to running along a vertical line in the plot of Fig. 10. The first nontrivial issue is that the crossover thicknesses which are observed in applied field deviate from the critical thicknesses in zero field.[2] The discrepancy is the stronger, the higher the field strength is. The complexity increases further if a film is studied which exhibits a canted spontaneous reorientation. A crossing field $H_{\rm cross}$ exists in such a film as clarified above. At $H=H_{\rm cross}$, the crossover thicknesses exchange their relative position. While for $H<H_{\rm cross}$ the situation is the same as expected from the zero-field case [d_0(coaxial) $<d_0$(in-plane); $K_{1s}>0$], it is reversed above that field strength. In the latter case ($H>H_{\rm cross}$), the SRT, when judged by the position of the crossover thicknesses, exhibits the same characteristics as a system with a spontaneous reorientation via the phase of coexistence. Consequently, if the crossover thicknesses are determined in a high-field experiment,[28] the same relation between the two d_L's will always be found, that is, the coaxial field configuration gives a higher crossover thickness (for $K_{1s}>0$). Inverting the argument, one cannot conclude from d_L(in-plane)/d_L(coaxial) <1 at some nonzero field that in zero field the system exhibits a SRT via the region of coexistence. To our knowledge, this subtlety has never been discussed or even noticed in the existing literature despite of its importance in avoiding confusion when experimental results on thin ferromagnetic film in applied field are interpreted. In any case, if the SRT and its crossover thickness are studied in a field, it is necessary to take care about measuring the field dependence of the latter (in the sense of the trend of variation with variation of the field). This would make it possible to obtain the linear dependence for $1/d_L$, determine whether a crossing field $H_{\rm cross}$ exists, and identify the relative positions of the intercepts.

Since the understanding of the expected shifts in the critical (crossover) thicknesses upon variation of the applied field is crucial to the correct interpretation and even setup of experiments on wedge-shaped magnetic films, we visualize the issue in Figs. 11(a), 11(b). The cases (a) and (b) correspond to systems where in zero field one finds coexistence of in-plane and vertical phases [case (a)] or a true canted phase [case (b)] over a certain thickness range. In-plane (left) and vertical (right) field configurations are envisaged in each case. Each sequence corresponds to fields of increasing strength, starting from the zero-field situation at the bottom. For systems exhibiting coexistence in zero field [Fig. 11(a)], the crossover thicknesses separating the competing phases run away from each other upon increasing the field strength in each configuration. For systems exhibiting the true canted phase in zero field [Fig. 11(b)], the crossover thicknesses move closer upon field increase, become equal at $H=H_{\rm cross}$ [cf. Eq. (15)], and run away for $H>H_{\rm cross}$. Thus, the literally *basic* cases in Figs. 11(a), 11(b), corresponding to zero field, leave their fingerprints and predetermine the tendency of variation of the crossover thicknesses upon an increase of the field in both configurations.

It is worth pointing out that the presented relations (11) and (12) for the linear functions $1/d_L(H)$ in both field configurations can also be used to analyze the set of anisotropy constants. Two intercepts and two slopes provide four conditions for the five generally unknown quantities K_{1b}, K_{2b}, K_{1s}, K_{2s}, and M. For systems in which a crossing as in Fig. 10(a,b) exists and can be experimentally detected at a certain field strength $H_{\rm cross}$, Eq. (15) provides for a fifth independent condition. Further options lie with the experimental detection of (some of) the nonlinear critical thicknesses and the consequent implementation of Eqs. (8) and (10). Any surplus information coming from the experimental side and leading to an overdetermined system of equations can be used as a consistency check on the whole procedure.

C. The nonlinear crossover thicknesses

These could be seen in experiment only if the trajectory crosses over between the two phases via the region of coexistence. If this is the case and the d_N's are taken as experimentally measurable quantities, Eqs. (8) and (10) provide additional conditions binding together the unknown material parameters listed in the previous paragraph.

VI. MAGNETIZATION PROFILES IN AN ULTRATHIN SYSTEM WITH A SPIN-REORIENTATION TRANSITION

The magnetization profile m_H is defined as the normalized component of magnetization along the direction of a given constant field:

$$m_H=\frac{M_H}{M}=\frac{M\ \cos(\theta-\phi)}{M}=\cos(\theta-\phi). \tag{16}$$

Hence, with a vertical field $\mathbf{H}_n$ we have $\phi=0$ and

$$m_n\equiv m_H(\text{coaxial})=\cos\ \theta, \tag{17}$$

while with an in-plane field $\mathbf{H}_p$ we have $\phi=\pi/2$ and

$$m_p\equiv m_H(\text{in-plane})=\sin\ \theta. \tag{18}$$

In other words, the profiles thus defined are nothing but x_n and x_p as defined in I. Consequently, the profiles are exhaustively described by the solutions to the cubic given in the Appendix of I. The regions of relevance for each particular solution have already been given in Figs. 3 and 4 of Ref. 1. When this knowledge is combined with the linearity of the thickness-driven trajectories in the (α,β) space, the profiles can be straightforwardly generated for any given system, i.e., for any given set of material parameters. We have already given examples of profiles (cf. Figs. 3, 4, and 6 above).

Rather generally, any profile $m_p(d)$ or $m_n(d)$ that encompasses a SRT would consist of a plateau of unit height which corresponds to the portion of the thickness-driven trajectory belonging to the conforming phase and a portion of monotonic variation with d. The crossover between the two regimes corresponds precisely to the crossover between the conforming and canted phases and takes place at the crossover thickness d_L or d_N.

If one considers the problem with the profiles from the other end and assumes that they can be measured together with the crossover thicknesses in experiment, one will be able to deduce further useful information in a number of ways. One could, e.g., find a sufficient number of independent relations to set up a procedure for the simultaneous determination and consistency checks of all material parameters relevant to the given SRT without recourse to data measured outside the given experiment. Here we give a very simple example for the construction of a self-consistent set of relations, but postpone more elaborate developments to a time when reliable experimental data will be available.

Consider the case of an ultrathin film in the vertical field configuration and assume that one has to deal with a situation specified by, say, the uppermost from among the trajectories in Fig. 8 which corresponds to a simple SRT at a crossover thickness d_L. With the expressions for the profile as found in the Appendix of I, one easily finds an asymptotic expression for $d\gg d_L$, i.e., for the far-end tail of the profile. This expression is best cast in the form

$$\frac{1}{m_n}\approx u_1\left(\frac{1}{d}\right)+v_1 \tag{19}$$

with $u_1=-2(K_{1s}+2K_{2s})/H$ and $v_1=2\Delta/H$. On the other hand, by Eq. (11),

$$\frac{1}{d_L}=u_2H+v_2 \tag{20}$$

with $u_2=-M/2K_{1s}$ and $v_2=\Delta/K_{1s}$. From the two linear plots (19) and (20) one derives four independent conditions (two slopes and two intercepts) for four quantities $(K_{1s},K_{2s};M,\Delta)$. The simple procedure illustrates how the *information inherent to the shape of the profiles*[29] can be used to complete the required set of independent relations. Although for this configuration the crossover thickness d_L is sensitive to first-order contributions only, the details of the shape help uncover the higher-order anisotropy contributions as might have been expected on intuitive physical grounds.

VII. FIELD vs THICKNESS PHASE DIAGRAM

The (H,d) representation of the phase diagram of a system undergoing a SRT is of most direct relevance. At the same time, it is connected with the largest loss of generality, since one has to assign definite values for quite a number of material parameters. Reasonable modelling is still possible with the help of the foregoing discussion. The general strategy to be pursued is also clear enough: One takes the defining equations for the borderlines from any of the different representations given above and in I. In the (α,β) representation, for instance, one starts with Eqs. (7),(8) for the coaxial configuration or with Eqs. (9),(10) for the in-plane configurations. The parameters are expressed as $\alpha[H,a(d)]$ and $\beta[H,b(d)]$. Every single equation defining a given phase boundary is solved for $H=H(d)$ or for $d=d(H)$ with the set of material constants as parameters. By inspection of the relevant equations, the linear boundaries remain linear and the nonlinear ones remain nonlinear.

Apart from the important differences, the appearance of a particular (H,d) diagram is quite similar to a corresponding

$(\bar{H},r)$ diagram, hence, we do not present illustrative plots.[30] Still, we find it important to give the expressions for the coordinates d_C and H_C of the tricritical point in (H,d) coordinates. These are

$$\text{coaxial: } d_C=\frac{K_{1s}-4K_{2s}}{\Delta+4K_{2b}}, \tag{21}$$

$$H_C=\frac{8}{M}\,\frac{\Delta\rho+4K_{2b}}{4\rho-1}; \tag{22}$$

$$\text{in-plane: } d_C=\frac{K_{1s}+6K_{2s}}{\Delta-6K_{2b}}, \tag{23}$$

$$H_C=-\frac{8}{M}\,\frac{\Delta\rho+K_{2b}}{6\rho+1}. \tag{24}$$

Here, we have introduced the ratio $\rho=\kappa_{2s}/\kappa_{1s}=K_{2s}/K_{1s}$ which is nothing but the slope of the linear trajectories defined above in Eq. (5).

VIII. SUMMARY

We have presented a detailed quantitative discussion of the influence of applied magnetic field on the characteristics of SRT's in thin ferromagnetic films. The two major configurations of vertical and in-plane directions of field have been treated on equal footing. Suitable representations of the problem have been developed. They allow to trace in any desired detail the various ways in which the field effects can be detected and described with variation of thickness at constant field or with variation of field at constant thickness. The phase diagrams in both field configurations exhibit a region of coexistence of canted and conforming phases for negative values of the second-order contribution $(b<0)$. The experimental view point was taken in demonstrating how the implementation of magnetic field and its variation can immediately tell on the behavior of the system in zero field. One can thus unambiguously identify the type of SRT as well as the signs of the different anisotropy contributions and their ratio.

The proposed systematics of possible SRT's builds upon the relevance and sign of the second-order anisotropy contribution and reveals the intrinsic connection of the spontaneous SRT's with those under field. The method of the thickness-driven flows in the anisotropy space of the system has been extended to account for the influence of the Zeeman unidirectional contribution. A simple and natural representation has been found which preserves the linear character of the anisotropy flows even for systems under field. When combined with the results of the stability analysis for the allowed phases, the concept provides an astonishingly lucid description of all aspects of a possible SRT. In particular, one is able to specify generic trajectories which cross one, two, or three phase boundaries. These cross points correspond to certain crossover thicknesses which are exhaustively described. Very generally, they are of two types, linear (d_L) and nonlinear (d_N), depending on the type of borderline which is being crossed by the linear trajectory. The conditions under which these points can be observed and the concommitant peculiarities in the behavior of the films have been discussed analytically and illustrated diagrammatically. The possibility for three crossover points (thicknesses) can be realized in a system which starts its thickness-driven evolution from within the region of coexistence.

The field dependence of the linear crossover thickness d_L is especially informative and sheds light on aspects which have remained unnoticed despite of their importance for the correct interpretation of SRT's in films under field. In particular, we have demonstrated that any applied field causes a shift of the critical thickness for a SRT. The $1/d_L$ vs H plots are linear and when examined *simultaneously* for both field configurations provide for insights into, and overview on, thin-film behavior under a field. It gives the experimentalist the opportunity to determine at least four out of five independent thin-film parameters related to anisotropy.

On the basis of this analysis, we have suggested different ways of how to perform experimental studies to the purpose of the determination of the complete set of relevant anisotropy parameters whose interplay underlies the specific way for a SRT in an applied field to show up. In particular, simple schemes are suggested for extracting the required sets of data from the shape of the magnetization profiles or from the calculated dependences for the crossover thicknesses d_L and d_N.

ACKNOWLEDGMENTS

Expert technical assistance by A. Kroder is gratefully acknowledged. Y.M. acknowledges support from the Max Planck Society and participation in Contract No. NSF Φ560.

*On leave from the CPCS Lab, Institute of Solid State Physics, Bulgarian Academy of Sciences, 1784 Sofia, Bulgaria.

[1] Y. T. Millev, H. P. Oepen, and J. Kirschner, preceding paper, Phys. Rev. B **57**, 5837 (1998).

[2] Y. Millev and J. Kirschner, Phys. Rev. B **54**, 4137 (1996). A factor of 2 is misplaced in Eq. (22), namely, the brackets in the denominator should enclose $2K_{2b}+K_{1b}$.

[3] U. Gradmann, Ann. Phys. (Leipzig) **17**, 91 (1966); U. Gradmann and J. Müller, Phys. Status Solidi **27**, 313 (1968).

[4] This factor is unity in SI.

[5] H. J. G. Draaisma and W. J. M. de Jonge, J. Appl. Phys. **64**, 3610 (1988); B. Heinrich, S. T. Purcell, J. R. Dutcher, K. B. Urquhart, J. F. Cochran, and A. S. Arrott, Phys. Rev. B **38**, 12 879 (1988); P. Jensen, Ann. Phys. (Leipzig) **6**, 317 (1997).

[6] E. F. Bertaut, *Magnetism*, edited by G. Rado and H. Suhl (Academic, New York, 1963), Vol. III, Chap. 7, pp. 351–194.

[7] M. N. Barber, in *Phase Transitions and Critical Phenomena*, edited by C. Domb and J. L. Lebowitz (Academic, London, 1983), pp. 145-266.

[8] U. Gradmann, in *Handbook of Magnetic Materials*, edited by K. H. J. Buschow (North-Holland, Amsterdam, 1993), Vol. 7, Chap. 1; *Ultrathin Magnetic Structures I*, edited by J. A. C. Bland and B. Heinrich (Springer, Berlin, 1994).

[9] D. S. Chuang, C. A. Ballentine, and R. C. O'Handley, Phys. Rev. B **49**, 15 084 (1994).

[10] Y. Millev, IEEE Trans. Magn. **32**, 4573 (1996).

[11] P. J. Jensen and K. H. Bennemann, Phys. Rev. B **52**, 16 012 (1995); Solid State Commun. **100**, 585 (1996); A. Moschel and

K. D. Usadel, Phys. Rev. B **51**, 16 111 (1995); A. Hucht, A. Moschel, and K. D. Usadel, J. Magn. Magn. Mater. **148**, 32 (1995); A. Hucht and K. D. Usadel, *ibid.* **156**, 423 (1996); A. B. Macisaac, J. P. Whitehead, K. De'Bell, and P. H. Poole, Phys. Rev. Lett. **77**, 739 (1996).

[12] This anisotropy-flow concept was proposed within an analysis of the temperature variation of bulk single-ion anisotropy, where a rather general theoretical description valid for a whole class of untrivial theories was developed [see Y. Millev and M. Fähnle, Phys. Rev. B **51**, 2937 (1995); **52**, 4336 (1995)]. Even there, the temperature dependence is not explicitly known and can be best described within a certain parametric approach.

[13] L. D. Landau and E. M. Lifshitz, *Electrodynamics of Continuous Media* (Pergamon, Oxford, 1960), Chap. 4 and 5.

[14] It must be noted that the latter is not a universally valid law. From the point of view of the anisotropy-flow concept, the linear character of the thickness-driven trajectories describing the evolution of the system in the suitably defined anisotropy space is not affected even with an arbitrary thickness dependence, provided that it is of the same functional form for *both* anisotropy orders (see Refs. 2 and 10).

[15] One cannot exclude the possibility that a criticality of higher order arises in some system, i.e., that both the first and second anisotropy contributions vanish at the same point. The first nonvanishing contribution would then be the third-order one in close analogy with multicritical phenomena in the theory of phase transitions.

[16] C. Chappert and P. Bruno, J. Appl. Phys. **64**, 5736 (1988).

[17] V. Grolier, J. Ferre, A. Maziewski, E. Stepanowicz, and D. Renard, J. Appl. Phys. **73**, 5939 (1993).

[18] H. Fritzsche, J. Kohlhepp, H. Elmers, and U. Gradmann, Phys. Rev. B **49**, 15 665 (1994).

[19] H. P. Oepen, M. Speckmann, Y. T. Millev, and J. Kirschner, Phys. Rev. B **55**, 2752 (1997); H. P. Oepen, Y. T. Millev, and J. Kirschner, J. Appl. Phys. **81**, 5044 (1997).

[20] M. Speckmann, H. P. Oepen, and H. Ibach, Phys. Rev. Lett. **75**, 2035 (1995).

[21] H. P. Oepen and J. Kirschner, Scanning Microsc. **5**, 1 (1991).

[22] L. G. Onoprienko, Fiz. Met. Metalloved. **19**, 481 (1965); A. I. Mitsek, N. P. Kolmakova, and D. I. Sirota, *ibid.* **38**, 35 (1974); G. Asti, in *Ferromagnetic Materials*, edited by K. H. J. Buschow and E. Wohlfarth (Elsevier, Amsterdam, 1990), Vol. 3, pp. 398–464; S. Nieber and H. Kronmüller, Phys. Status Solidi B **165**, 503 (1991).

[23] Since $\kappa_{2s}/\kappa_{1s}=K_{2s}/K_{1s}$, it is only the uniformity of notations that justifies the seemingly superfluous form given in the text. It should not disguise the fact that the slope of the linear trajectories is given, even with field, by the plain ratio of the surface constants. For Co/Au(111) (Ref. 19), one finds that this ratio is a small quantity ($-7/40$ for annealed wedges, $\approx -1/5$ for as-grown wedges) which is why the thickness-trajectory of the system in the anisotropy space is rather flat. The same feature obviously holds for the same system in applied field.

[24] A further step to an exhaustive description would be to attempt an analytic description of the phase diagram in the (α,β) representation for *any* orientation of the applied field and not only for $\phi=0$ (coaxial) or $\phi=\pi/2$ (in-plane) (ϕ is the angle between **H** and **n**). Pictorially, one has the first and the last pages in a book whose pages are labeled by, say, equidistant ϕ's from within the interval $[0,\pi/2]$. For a given system in a field of fixed magnitude the trajectory in the (α,β) space can be engraved on the cover and will be valid for every single page. More formally, an explicit analytic description should allow one to trace the continuous transformation of the borderlines under the variation of direction of **H** ($\phi\in[0,\pi/2]$) at a fixed magnitude H.

[25] An alternative convention for ''initial'' and ''final'' in the present context would be to always take the *conforming state* as the initial state. This would, however, introduce unnecessary confusion when discussing the different field configurations.

[26] Y. Millev and M. Fähnle, IEEE Trans. Magn. **32**, 4743 (1996).

[27] The discussion holds true for $K_{1s}<0$ with all the inequalities reversed.

[28] In this instance, ''high fields'' are those of strength higher than $H_{\rm cross}$; the latter is determined again by the anisotropy parameters as given in Eq. (15).

[29] In this case, the *asymptotic* shape has been taken into consideration.

[30] Besides, as has just been remarked, one needs all details about the involved quantities, quite unlike the rather general $(\overline{H},r)$ presentation.